Hierarchical Bayesian Spatiotemporal Analysis of Revascularization Odds using Smoothing Splines

Giovani L. Silva, C. B. Dean, Théophile Niyonsenga, Alain Vanasse

Departamento de Matemática
Instituto Superior Técnico
Lisboa, Portugal
Preprint 2/2006

http://preprint.math.ist.utl.pt/?serie=dmist

Hierarchical Bayesian Spatiotemporal Analysis of Revascularization Odds using Smoothing Splines

Giovani L. Silva

Departamento de Matemática - IST, Universidade Técnica de Lisboa
Av. Rovisco Pais, 1, 1049-001 Lisboa, Portugal

C. B. Dean

Department of Statistics and Actuarial Science, Simon Fraser University
8888 University Drive, Burnaby, BC V5A 1S6, Canada

Théophile Niyonsenga

College of Health and Urban Affairs, Florida International University, University Park
HLS 683, 11200 SW 8th Street Miami, FL 33199, U.S.A.

and

Alain Vanasse

Département de Médecine de Famille, Groupe PRIMUS, Faculté de Médecine
Université de Sherbrooke, 3001, 12e Avenue Nord, Sherbrooke, Québec J1H 5N4, Canada

Abstract

Hierarchical Bayesian models are proposed for over-dispersed longitudinal spatially correlated binomial data. This class of models accounts for correlation among regions by using random effects and allows a flexible modelling of spatiotemporal odds by using smoothing splines. The aim is (i) to develop models which will identify temporal trends and produce smoothed maps including regional effects of odds, (ii) to specify Monte Carlo Markov Chain inference for fitting such models, (iii) to study the sensitivity of such Bayesian binomial spline spatiotemporal analyses to prior assumptions, and (iv) to compare mechanisms for assessing goodness-of-fit. An analysis of regional variation for revascularization odds of patients hospitalized for acute coronary syndrome in Quebec motivates and illustrates the methods developed.

Keywords: Disease mapping, Hierarchical Bayesian model, Spatiotemporal smoothing, MCMC methods, Binomial data.

1 Introduction

Describing the spatiotemporal disparities in health utilization is critical for health systems analysis and for assessing the distributive impact within systems of public policies in relation to spatial or health status inequalities. Studies involving rare events are common in the population health context and many methodological advances have been made for spatiotemporal studies of population health using the generalized linear or additive mixed Poisson frameworks. In studies of health system utilization the Poisson baseline structure may not be appropriate as events, referring to specific choices of medical procedures for individuals diagnosed with a disease, are typically not rare or contagious. We consider here spatiotemporal modelling of odds and, importantly, reflect on how Bayesian prior assumptions affect rates and risks in the mixed binomial spatial setting.

This article presents a Bayesian approach of a flexible spatial generalized additive mixed model developed by MacNab and Dean (2001) and adapted here for the spatiotemporal analysis of health utilization outcomes and binomial data. In particular, we consider the spatial and temporal trends in the annual number of revascularizations at index hospitalization for individuals diagnosed with acute coronary syndrome between 1993 and 2000 in the province of Quebec in Canada. Revascularization includes angioplasty and aortocoronary bypass. Index hospitalization refers to the first hospitalization for acute coronary syndrome. Revascularizations at index hospitalization have been increasing because of recent changes in guidelines concerning these treatments. This study monitors the sharply and steadily changing trends.

The use of B-splines in Bayesian spatiotemporal models is another relevant aspect of this work. Spline smoothing may reveal nonlinear temporal effects for both the overall temporal and small-area regional temporal components. B-splines have an advantage of being easily incorporated into the modelling of temporal components; in addition, estimation is computationally straightforward. However, other basis functions could also be used, *e.g.*, P-splines, which are low-order basis splines, with a penalty to avoid undersmoothing. Baladandayuthapani, Mallick and Carrol (2005) study spatially adaptive Bayesian penalized regression splines for Gaussian response data; Holmes and Mallick (2003) present Bayesian generalized nonlinear models for univariate and multivariate non-Gaussian response data, including a random residual component for the linear predictor and basis splines with the number and location

of the knots treated as random.

Lawson *et al.* (1999) provide a comprehensive review of disease mapping, while Banerjee, Carlin and Gelfand (2004) and the references therein present recent substantial work in hierarchical Bayesian models for spatial and spatiotemporal data. MacNab (2003) has discussed spatial modelling for non-rare diseases using a binomial framework. Knorr-Held and Besag (1998) model longitudinal spatial binomial data with time incorporated as a categorical variable and emphasize the role of time and space-varying covariate effects. MacNab and Dean (2001) and Waller *et al.* (1997) consider two different approaches to spatiotemporal modelling and analysis within the Poisson framework. The former uses smoothing splines to isolate temporal trends, while the latter augments the autoregressive formulation of the spatial correlation with an autoregressive temporal correlation in a similar vein as for traditional time series analysis, but of count data. Here we also use smoothing splines, though an autoregressive temporal analysis could be considered in a complementary analysis to that of Waller *et al.* (1997).

In addition, it is important to study inference for additive binomial models in mapping utilization data, especially when a Poisson approximation to the binomial might not be appropriate. With mixed Poisson models, approximate methods of inference, for example penalized quasi-likelihood (Breslow and Clayton, 1993), seem to work well (Lin and Breslow, 1996). Indeed, this was used by MacNab and Dean (2001) for their spatiotemporal analysis using the sort of additive models proposed here. However such methods have been documented to perform poorly for the binomial setting (Breslow and Clayton, 1993; Lin and Breslow, 1996). We adopt here, instead, the use of Bayesian inference and complement this with a study of the influence of prior assumptions to provide confident recommendations on the flexibility, usefulness and appropriateness of the Bayesian formulation in this context. Due to the complexity of the proposed model, we make inference by using Markov chain Monte Carlo (MCMC) methods which are very popular in Bayesian approaches for spatial analyses.

The rest of the article is organized as follows. Section 2 develops the spatiotemporal odds model as a generalized additive binomial model. In Section 3 we discuss Bayesian inference using MCMC methods and techniques for model comparison. An analysis of revascularization trends in Quebec is presented in Section 4 with a corresponding evaluation in Section 5 of sensitivity of such types of analyses to prior assumptions in the binomial context. Section 6 provides a discussion and recom-

mendations.

2 Spatiotemporal Odds Model

Let y_{it} denote the count of the number of what will be broadly termed "successes" out of n_{it} "trials" for region i in time t, $i=1,\ldots,n$, $t=1,\ldots,T$. In health utilization studies, n_{it} would refer to the size of a population for whom some binary outcome was recorded at the individual level; y_{it} equals the total number of individuals for whom the binary value is unity, indicating a service utilization in the period considered. Conditional on θ_{it}, we assume y_{it} has a binomial distribution with parameters n_{it} and θ_{it}, where θ denotes the probability of success. A Poisson approximation to the binomial might be appropriate if rates are rare; usually spatial analyses of rates make that assumption. In many health utilization settings, rates are non-rare.

A flexible and broad additive spatiotemporal model is given by

$$logit\ \theta_{it} \equiv \ln(\theta_{it}/(1-\theta_{it})) = S_0^\star(t) + S_i^\star(t), \tag{1}$$

where $S_0^\star(t)$ represents the overall temporal trend in the log odds over the whole region and $S_i^\star(t)$ represents the small-area specific trends over and above the overall trend. With time as centered, we formulate $S_0^\star(t) = \alpha_0 + S_0(t)$, where $S_0(t)$ takes the flexible form of a spline without intercept and, in this case, α_0 represents the overall mean log odds over the region and time period studied. Similarly, region-specific effects are defined as $S_i^\star(t) = S_i(t) + b_i + h_i$, $S_i(t)$ being a linear trend or an area-specific spline, b_i a spatially correlated random effect, and h_i an independent random effect. Covariates may also be included in model (1) additively, as well as age-group effects, which would give rise to extensions of the current model. Implementation of such extensions is straightforward using the general framework provided below.

Assuming a cubic spline without intercept and with one inner knot for $S_0(t)$ and a linear trend for $S_i(t)$, one obtains, for example, a simple flexible model from (1):

$$logit\ \theta_{it} = \alpha_0 + \sum_{k=1}^{4} \beta_{0k} p_k(t) + \delta_i\, t + b_i + h_i, \tag{2}$$

where $p_k(\cdot)$, $k=1,\ldots,4$, are the spline basis functions and β_{0k} the corresponding coefficients, and δ_i is the linear temporal effect relating to the ith region, $i=1,\ldots,n$. B-spline smoothing is proposed for describing the nonlinear temporal effects and

may be used for both the overall temporal $S_0(t)$ and the regional temporal $S_i(t)$ components. In this case, (2) is replaced with

$$logit\ \theta_{it} = \alpha_0 + \sum_{k=1}^{4} \beta_{0k} p_k(t) + \sum_{k=1}^{4} \beta_{ik} p_k(t) + b_i + h_i, \tag{3}$$

where β_{ik}, $k = 1, \ldots, 4$, are random effects that correspond to the temporal effects at the regional level. However, model (2) offers reasonable flexibility in modelling these temporal effects, and is parsimonious especially in terms of its interpretation. It may be particularly useful for exploratory analysis of trends, where the time period under observation is less than 10 years, and if diagnostics on a small-area level do not indicate peaks or troughs.

3 Bayesian Inference and Model Comparison

Recent developments in empirical Bayes and Bayesian hierarchical modelling have made it possible to obtain stable estimators for mortality rates in small areas by using information from all areas to derive estimates for individual areas. Banerjee, Carlin and Gelfand (2004) provide a comprehensive review of hierarchical Bayesian models for spatial and spatiotemporal data, including Bayesian lattice (areal data) modeling and multivariate spatial responses.

3.1 Prior assumptions

In the previous section, we assumed the spatial random small-area regional effect is the sum of a structured (b_i) and unstructured (h_i) component. Besag, York and Mollié (1991) argue that structure with a convolution prior distribution allows that the data decide how much of the residual disease risk is due to both spatially structured variation and unstructured over-dispersion. One typically assumes independence and a set of exchangeable Normal prior distributions for the unstructured random effects, *i.e.*, $h_i \sim N(0, \sigma_h^2)$, $i = 1, \ldots, n$, independently, where the symbol "$\sim$" means "distributed as" and $N(m, v^2)$ denotes a normal distribution with mean m and variance v^2. It is worth noting that the hyperparameter σ_h^2 controls the amount of excess heterogeneity. Moreover, if a linear trend $S_i(t) = \delta_i\, t$ is postulated for $S_i^{\star}(t)$ in (1), as in model (2), one may also assume that $\delta_i \sim N(0, \sigma_\delta^2)$, $i = 1, \ldots, n$, independently, and independent of spatial random effects b_i and h_i. When considering cubic

B-splines for $S_0(t)$ and $S_i(t)$, the corresponding spline basis functions β_{0k} and β_{ik} would be assigned independent normal distributions with zero mean and variances v_k^2 and σ_k^2, respectively, $k=1,\ldots,4$.

The conditional autoregressive model is adopted for the spatial random effects (Besag, York and Mollié, 1991) with the joint density of the vector $\mathbf{b} = (b_1,\ldots,b_n)$ being a multivariate normal distribution with mean vector $\mathbf{0}$ and inverse covariance matrix $\sigma_b^2\,\mathbf{Q}$, where $\mathbf{Q} = \{Q_{ij}\}$ is a matrix with entries specified by the spatial correlation postulated and σ_b^2 is the variance parameter that controls the amount of spatial similarity. A simple structure expressed conditionally proposes that $b_i|\mathbf{b}_{-i},\sigma_b^2 \sim N(\bar{b}_i,\sigma_b^2/n_i)$, where $\bar{b}_i = \sum_{j\in\mathcal{N}_i} b_j/n_i$, $\mathcal{N}_i$ denotes the set of "labels" of the "neighbours" of region i, n_i is the number of neighbours of region i, and $\mathbf{b}_{-i}$ denotes $(b_1,\ldots,b_{i-1},b_{i+1},\ldots,b_n)$. In this case, $\mathbf{Q}$ has diagonal element $Q_{ii} = 1/n_i$ and the off-diagonal element Q_{ij} is 1 if regions i and j are neighbours and 0 otherwise, $i,j=1,\ldots,n$. This conditional autoregressive model (the so-called "intrinsic CAR model") often serves as a useful approximation to the complicated correlation structures which may underlie the responses. In the health utilization context, neighbours might be areas which are adjoining, or which share bridges. Other complicated spatial formulations might have correlations depend on distance from a point source and these are useful in specific monitoring contexts.

For the hyperparameters σ_b^2 and σ_h^2 (the variance components), one usually assigns an inverse gamma prior, *i.e.*, $\sigma_b^2 \sim IG(c_1,d_1)$ and $\sigma_h^2 \sim IG(c_2,d_2)$, where $IG(c,d)$ denotes an inverse gamma distribution with shape parameter c and scale parameter d, whose kernel density is equal to $x^{-(c+1)}\exp(-d/x)$, $x>0$. If $S_i(t) = \delta_i\,t$ with $\delta_i \sim N(0,\sigma_\delta^2)$, one may also consider $\sigma_\delta^2 \sim IG(c_3,d_3)$, whereas for $S_i(t) = \sum_k \beta_{ik}p_k(t)$ with $\beta_{ik} \sim N(0,\sigma_k^2)$, $\sigma_k^2 \sim IG(c_{4k},d_{4k})$, $k=1,\ldots,4$, $i=1,\ldots,n$. In fact, these inverse gamma priors, as well as the normal priors for the B-spline coefficients β_{0k}'s, are usually assigned highly dispersed, but proper, priors.

3.2 Joint posterior and MCMC methods

Assuming independence of the model hyperparameters, the joint posterior density for model (2) is then proportional to

$$\prod_{i=1}^{n}\prod_{t=1}^{T}\left[{\theta_{it}}^{y_{it}}(1-\theta_{it})^{n_{it}-y_{it}}\right] \times \left(\frac{1}{\sigma_b^2}\right)^{\frac{n}{2}+c_1+1} \exp\left(-\frac{1}{\sigma_b^2}\left(d_1+\sum_{i=1}^{n}\frac{n_i(b_i-\bar{b}_i)^2}{2}\right)\right)$$
$$\times \left(\frac{1}{\sigma_h^2}\right)^{\frac{n}{2}+c_2+1} \exp\left(-\frac{1}{\sigma_h^2}\left(d_2+\sum_{i=1}^{n}\frac{h_i^2}{2}\right)\right) \times \exp\left(-\sum_{k=1}^{4}\frac{\beta_{0k}^2}{2\,v_k^2}\right) \times \prod_{k=1}^{4}[v_k^2] \times [\alpha_0] \quad (4)$$
$$\times \left(\frac{1}{\sigma_\delta^2}\right)^{\frac{n}{2}+c_3+1} \exp\left(-\frac{1}{\sigma_\delta^2}\left(d_3+\sum_{i=1}^{n}\frac{\delta_i^2}{2}\right)\right),$$

where $[\cdot]$ indicates the prior density. In order to ensure that the intrinsic CAR model is identifiable, Besag and Kooperberg (1995) suggest constraining the random effects to sum to zero, and using a flat prior on the whole real line for the intercept, α_0, as an alternative to the unconstrained parameterisation with no separate intercept. The posterior (4) would need slight modification according to the selected model in (1). For instance, assuming also a cubic spline without intercept for $S_i(t)$, *i.e.*, model (3), the distribution (4) only changes its third line which is replaced with $\prod_{k=1}^{4}(1/\sigma_k^2)^{\frac{n}{2}+c_{4k}+1}\exp(-(1/\sigma_k^2)(d_{4k}+\sum_{i=1}^{n}(\beta_{ik}^2/2)))$.

The joint posterior distribution (4), including its version for model (3), is awkward to work with, since the marginal posterior distributions of some parameters are not easy to obtain explicitly. Nevertheless, these posteriors can be evaluated using Markov chain Monte Carlo (MCMC) methods (see, *e.g.*, Chen, Shao and Ibrahim, 2000). In particular Gibbs sampling works by iteratively drawing samples for each parameter from the corresponding full conditional distribution, which is the posterior distribution conditional upon current values of all other parameters.

Let $\boldsymbol{\theta}$ be the vector of the model parameters, with elements b_i, h_i, β_{0k}, α_0, σ_b^2, σ_h^2, and v_k^2, including δ_i and σ_δ^2 for model (2) or β_{ik} and σ_k^2 for model (3), $k=1,\ldots,4$, $i=1,\ldots,n$. Denote $\boldsymbol{\theta}_{-j}$ the vector $\boldsymbol{\theta}$ without the its component j. From the joint posterior (4), the full conditional posterior distributions, denoted by $[j|\boldsymbol{\theta}_{-j}]$, are given by:

i) $[b_i|\boldsymbol{\theta}_{-b_i}] \propto \exp(b_i\sum_t y_{it} - \sum_t n_{it}\log A_{it} - \frac{n_i}{2\sigma_b^2}(b_i-\bar{b}_i)^2)$, $i=1,\ldots,n$;

ii) $\sigma_b^2|\boldsymbol{\theta}_{-\sigma_b^2} \sim IG(c_1+n/2,\, d_1+\sum_i n_i(b_i-\bar{b}_i)^2/2)$;

iii) $[h_i|\boldsymbol{\theta}_{-h_i}] \propto \exp(h_i\sum_t y_{it} - \sum_t n_{it}\log A_{it} - h_i^2/(2\sigma_h^2))$, $i=1,\ldots,n$;

iv) $\sigma_h^2|\boldsymbol{\theta}_{-\sigma_h^2} \sim IG(c_2 + n/2,\, d_2 + \sum_i h_i^2/2)$;

v) $[\beta_{0k}|\boldsymbol{\theta}_{-\beta_{0k}}] \propto \exp(\beta_{0k} \sum_t p_k(t) \sum_i y_{it} - \sum_i \sum_t n_{it} \log A_{it} - \beta_{0k}^2/(2v_k^2)$, $k=1,\ldots,4$;

vi) $[\alpha_0|\boldsymbol{\theta}_{-\alpha_0}] \propto \exp(-\alpha_0 \sum_i \sum_t y_{it} - \sum_i \sum_t n_{it} \log A_{it}) \times [\alpha_0]$;

vii) $[\delta_i|\boldsymbol{\theta}_{-\delta_i}] \propto \exp(\delta_i \sum_t t\, y_{it} - \sum_t n_{it} \log A_{it} - \delta_i^2/(2\sigma_\delta^2))$ for model (2) or $[\beta_{ik}|\boldsymbol{\theta}_{-\beta_{ik}}]$ $\propto \exp(\beta_{ik} \sum_t p_k(t) y_{it} - \sum_t n_{it} \log A_{it} - \beta_{ik}^2/(2\sigma_k^2))$, $k=1,\ldots,4$, for model (3), $i=1,\ldots,n$;

viii) $\sigma_\delta^2|\boldsymbol{\theta}_{-\sigma_\delta^2} \sim IG(c_3 + n/2,\, d_3 + \sum_i \delta_i^2/2)$ for model (2), whereas for model (2) $\sigma_k^2|\boldsymbol{\theta}_{-\sigma_k^2} \sim IG(c_{4k} + n/2,\, d_{4k} + \sum_i \beta_{ik}^2/2)$, $k=1,\ldots,4$,

ix) $[v_k^2|\boldsymbol{\theta}_{-v_k^2}] \propto \exp(\sum_k (k \ln v_k^2)/2 - \sum_k \alpha_k^2/(2v_k^2)) \times [v_k^2]$, $k=1,\ldots,4$,

where $A_{it} = 1 + \exp(\alpha_0 + \sum_k \beta_{0k} p_k(t) + S_i(t) + b_i + h_i)$, $i=1,\ldots,n$, $t=1,\ldots,T$.

Sampling values from the conditional posteriors above is straightforward, especially when using the Metropolis-Hastings algorithm (see, *e.g.*, Chen, Shao and Ibrahim, 2000). Implementation in many statistical programming packages is not difficult. Alternatively, Gibbs sampling via the software GeoBUGS by Thomas *et al.* (2004) could be used; this provides estimates of posterior quantities of interest for the current model, namely, the relative spatial odds for area i, $\exp(b_i + h_i)$. However, note that the practical implementation of these techniques requires particular care in this scenario, since the models involve many parameters which are weakly identified.

3.3 Model comparison

An important issue is to choose among postulated sub-models of model (1), especially because certain Bayesian model choice techniques are not applicable here. For example, Bayes factors are not interpretable with flat or CAR priors for the model parameters. In contrast with most papers related to Bayesian models for disease mapping, Waller *et al.* (1997) handle model selection by calculating the expected predictive deviance in the context of choosing amongst various Poisson spatiotemporal models of lung cancer mortality. In the current case, the deviance of a binomial likelihood, which is given by

$$D(\theta_{it}) \;=\; 2\sum_{i=1}^{n}\sum_{t=1}^{T}\left(y_{it}\log\left(\frac{y_{it}(1-\theta_{it})}{\theta_{it}(n_{it}-y_{it})}\right) + n_{it}\log\left(\frac{1-(y_{it}/n_{it})}{1-\theta_{it}}\right)\right), \qquad (5)$$

may be routinely evaluated via MCMC methods, with θ_{it} replaced with its current value in each iteration of the simulated sample.

Another summary measure of model comparison, which is easily evaluated with MCMC methods, is based on the conditional predictive ordinate (CPO), defined for the ith region at time t as

$$CPO_{it} \equiv f(y_{it}|\mathbf{y}_{-it}) = \int f(y_{it}|\boldsymbol{\theta}, \mathbf{y}_{-it}) \, [\boldsymbol{\theta}|\mathbf{y}_{-it}] \, d\boldsymbol{\theta} \,, \tag{6}$$

where $\mathbf{y}_{-it}$ is the vector of the observed data $\mathbf{y}$ without the observation y_{it}, and $f(\cdot)$ and $[\cdot|\cdot]$ denote the conditional sampling and posterior distributions, respectively. A low value for $\sum_{it} \log CPO_{it}$ indicates agreement between the observations and the model. The calculation of (6) involves evaluating the posterior for different subsets of the observed data, defined by dropping out each region i and time t. That can be arduous, especially for large data sets. Alternatively, the quantity (6) may be evaluated by MCMC methods using $g\{\sum_{j=1}^{g}\{f(y_{it}|\boldsymbol{\theta}_j)\}^{-1}\}^{-1}$ from the posterior with only the dataset $\mathbf{y}$, where g is the number of iterations of the simulated sample and $\boldsymbol{\theta}_j$ is the value of $\boldsymbol{\theta}$ obtained in the jth iteration of the simulated sample. Care must be employed when interpreting the measure (6) as spatiotemporal data are not typically independent.

An alternative measure, proposed by Spiegelhalter *et al.* (2002), for comparing complex models like model (1) is called the Deviance Information Criterion (DIC). That measure is a generalization of the Akaike information criterion (AIC) which handles hierarchical Bayesian models of any degree of complexity, and is computed as the sum of two components: the expected posterior deviance (5), measuring the goodness of fit, and the effective number of parameters (p_D), measuring complexity of the model. Note that p_D penalizes increasing model complexity and is calculated via $p_D = \bar{D} - D(\bar{\theta}_{it})$. Consequently, the measure is often expressed as

$$DIC = 2\,\overline{D(\theta_{it})} - D(\overline{\theta}_{it}), \tag{7}$$

where $\overline{D(\theta_{it})}$ and $\overline{\theta}_{it}$ denote the posterior mean of the deviance (5) and the model parameter θ_{it}, respectively.

In Bayesian estimation of disease mapping, it is also important to choose a suitable combination of hyperparameters σ_b^2 and σ_h^2, as well as σ_δ^2 or σ_k^2, as required. Of course, in most cases, the data dominate the prior and hence there is little sensitivity to the values of the hyperparameters chosen. Prior sensitivity, choices of models and priors at stages two and three of the hierarchy are discussed in detail in Pascutto

et al. (2000) and the references therein. We will carefully investigate choice of prior through a sensitivity study for the analysis of the revascularization data in Section 5. We also discuss prior sensitivity broadly in the discussion.

4 Analysis of Revascularization Odds

All patients 25 years and older hospitalised for acute coronary syndrome (ACS) including hospital transfers between January 1st, 1993 and December 31st, 2000 in the province of Quebec in Canada are considered in this cohort. The first such hospitalization within a window of 2 years prior to 1993 is used to identify index hospitalization. Technically, index hospitalization refers to no previous hospitalization for ACS dating back to 1991. For each case of an index hospitalization, the response is recorded as a treatment of revascularization through angioplasty or aortocoronary bypass. Individuals are stratified by gender and local health area (LHA) of residence. There are 139 LHAs in Quebec.

Two covariates were initially considered at LHA level: material deprivation index (MDI) and social deprivation index (SDI). Deprivation can be interpreted as a disadvantage relative to the local area or the whole society to which an individual belongs. Material deprivation results from a removal of the goods and conveniences related to modern lifestyle, being often associated with "poverty". Social deprivation refers to the degree of social network among individuals, such as isolation or cohesion in the family or workplace (Pampalon and Raymond, 2000). The first, second and third quartiles for MDI (SDI, respectively) with regard to the 139 LHAs in that period were 0.101 (0.020), 0.234 (0.084) and 0.428 (0.250), with MDI having a larger range than SDI among these LHAs. However, neither of them was significant in any analysis.

The means of the annual counts of both revascularization and ACS for each LHA range from (0.6,273.8) and (3.0,988.1), respectively. Matagami and Murdochville have the smallest means of both revascularization (about 0.7) and ACS (about 3) counts. The two largest annual count means of both revascularization and ACS correspond to Charlesbourg and Chambly-Carignan-Marieville, whose associated values are approximately 273.8 and 176.6 for revascularization, and 988.1 and 803.4 for ACS, respectively. These means are considerably larger than the overall annual means for revascularization (about 32) and ACS (about 129) counts. Moreover,

means of the rates of revascularization shown in Table 1 are increasing over time both for males and for females, with rates for females lower than those for males.

Because some interactions with gender were evident, analyses were stratified by gender. Several spatiotemporal models of the form (1) were fitted for analysing the odds of revascularization. For instance, the simple linear temporal trend model was considered, denoted by $M1$ and defined as $logit\,\theta_{it} = \alpha_0 + \beta\, t$. Estimates of the linear trend effect β indicate a significant increasing trend ($\exp(\hat{\beta}) \approx 1.16$) in the odds of revascularization over time for this period for both males and females. Note that MCMC samples of size 10,000 were obtained for $M1$ and other models considered, taking every 5th iteration of the simulated sequence, after 5,000 iterations of burn-in. A study of convergence of the samples was carried out using several diagnostic methods implemented in the Bayesian Output Analysis (BOA) program (Smith, 2004). None of them showed any distinguishing features, apart from convergence being a bit slow.

Table 2 lists $M1$ and other models which were found useful in our exploration of the data. These sub-models of the spatiotemporal model (1) have a increasing level of complexity, *e.g.*, model $M2$ is the simple linear trend model $M1$ plus a linear regional (LHA) temporal component ($S_i(t) = \delta_i\, t$), and spatially structured (b_i) and unstructured (h_i) components; models $M3$ and $M4$ are defined in (2) and (3), respectively. In order to compare competing models, we calculated the measures of overall fit (5), (6) and (7), as well as the posterior mean of the Pearson function Q_P. Based on these values listed in Table 2, models $M3$ and $M4$ seem somewhat better than the other two, particularly over $M1$ which includes no spatial random effects. There is evidence of both a trend and spatial variation in revascularization odds. The best model as defined by each measure is underlined in Table 2 and is identified consistently as $M4$. Here, we also choose to make inference from model $M3$, since the linear LHA temporal trend (δ_i) offers a simple interpretation of the spatiotemporal disparities in health system utilization at the small-area level, and the fit is comparable to that of $M4$.

Note that though CPO in (6) has a well-documented instability, no convergence problems were observed for any of the model comparison measures in our context. There is also a concordance amongst them across the models, *i.e.*, the reduction in the measures from $M1$ to $M4$ seems generally to have similar magnitude both for males and for females, apart from $-\sum_i \log CPO_i$ when comparing $M2$ and $M3$ for females. This measure favours $M2$ slightly in contrast to the others. Overall,

though, the agreement in these measures for the comparisons considered is very good.

Figure 1 displays the estimates of the overall odds of revascularization at index hospitalization for models $M1$, $M3$ and $M4$; estimates are provided in Table 3. Specifically, that rate is $\exp(\alpha_0 + \sum_k \beta_{0k} p_k(t))$ for models $M3$ and $M4$, and $\exp(\alpha_0 + \beta\, t)$ for model $M1$. Over this period, departures from linearity are observed in the overall increases in revascularization odds for both males and females with slower than the overall linear increase in the early years, especially for males. The change in the estimated probability of revascularization shows a sharp increase from January 1st in 1993 to December 31st in 2000 based on these three models. Estimates of the overall temporal trend derived from models $M3$ and $M4$ are quite close.

Table 4 provides estimates of the variance components for models $M3$ and $M4$, including estimates of the quantity $\sigma^2_{b.tot} = \sigma^2_b/(\sigma^2_b + \sigma^2_h)$, which is interpreted as the relative importance of the spatially correlated variance component versus the total spatial variance component. Recall, however, that the variance of spatially correlated random effect is not simply σ^2_b, as this refers to the conditional variance of $b_i|\mathbf{b}_{-i}$. Here, this measure is useful informally. The credible intervals are highest posterior density (HPD) intervals and were obtained via the BOA Program (Smith, 2004) by using Chen and Saho's technique (see, *e.g.*, Chen, Shao and Ibrahim, 2000). Both models identify significant heterogeneity in this data, but the greatest influence on heterogeneity arises from spatial correlation, which has a relative importance in relation to the total spatially variance of about 98% (males) and 94% (females) for model $M4$ and 96% (males) and 95% (females) for model $M3$. One might also note that there is less spatial variability in revascularization for females, as well as lower odds for women generally as seen in Table 3.

In order to identify regions with significant LHA temporal trends, 95% HPD credible intervals were also obtained for $\exp(\delta_i)$ based on model $M3$. That quantity represents the ratio of the odds of revascularization over two consecutive years, or the factor of increase in the odds of revascularization from one year to the next, for a specific region. Figure 2 shows plots of these credible intervals for males and females by LHA in increasing order of the trend effect. Clearly these factors can be quite substantial. Gatineau and Hull stand out with large values of the trend effect for both genders, whereas L'Amiante and L'Islet have the lowest significant LHA temporal effects for males and females, respectively. The regions with the highest and lowest ten posterior mean estimates are listed in Table 5 according to increasing

order of LHA temporal trend and identify the large discrepancy between the odds for Gatineau and Hull and the remaining regions.

Figure 3 maps the LHA temporal trend ($\exp(\delta_i)$) estimates obtained from the fit of model $M3$ by gender, while Figures 4 and 5 map the spatial variation in 1993 and 2000 based on model $M4$ for males and females, respectively. The Montreal metropolitan region is highlighted in the inset of these maps because that is the most populous area in the province of Quebec and the corresponding LHAs cannot be easily seen in the main maps. The cutpoints for the colour shading in the legend divide the risk and trend effects into equal quantiles. From Figure 3, we can observe that the highest LHA temporal trends are located in the south-western regions both for males and females, specifically in the greater Ottawa and Montreal cities (see also Table 5).

The spatial distribution of the LHA effects over time is here mapped as $\exp(S_i(t) + b_i + h_i)$; this provides identification of those regions experiencing large differing LHA temporal effects with respect to the overall spline. For male patients, there is a change from 1993 to 2000 in which regions had the highest estimates (see Figure 4). In particular, Chomedey had the highest estimate (1.852) in 1993 which decreased to 1.42 in 2000, whereas Saint-Louis-du-Parc had a modest estimate of 1.30 in 1993 which escalated to the highest values of 1.825 in 2000. Similar sharp changes also occurred for females; specifically, Petite Patrie had a increasing trend from 1.136 in 1993 to the largest value of 1.708 in 2000. The largest LHA effect estimates are typically in the vicinity of greater Montreal. Hull and Gatineau experienced the sharpest increase in LHA temporal trend effects. However, revascularization odds estimates for these regions are still only modest at the end of the period for both males and females.

Plots of the revascularization odds estimates for six selected health areas, including Hull and Gatineau, are provided in Figures 6 and 7 for males and females over time. Standardized crude odds are defined by $y_{it}/[(n_{it}-y_{it})o_t]$, where $o_t = \sum_i y_{it}/\sum_i (n_{it}-y_{it})$, whereas other estimates are $\exp(\delta_i t+b_i+h_i)$ $(M3)$ and $\exp(\sum_k \beta_{ik}p_k(t)+b_i+h_i)$ $(M4)$. There are abrupt increases evident after a changepoint (see Hull and Gatineau at 1996) which could be related to movement of key surgeons and specific changes in guidelines for management of the disease which took effect in 1996. It would be interesting to complement this study with an investigation of surgeon effects.

5 Sensitivity Analysis

In hierarchical models, the hyperprior distributions of the variance components (σ^2) are generally set to be vague to allow learning from the data. Specifically, the gamma distribution with scale and shape parameters equal to 0.001 has often been used as a default prior for the precision of the random effects ($1/\sigma^2$). Kelsall and Wakefield (1999) suggest the use of the gamma with scale parameter 0.5 and shape parameter 0.0005 for modeling the precision of the spatial random effects in a CAR model, and argue that this prior is a reasonable choice for estimation of relative risks within the class of gamma priors. The former prior may lead to imposition of a hypothetical spatial effect because most of the prior mass is away from zero. The latter prior expresses the belief that the distribution of the standard deviation of the random effects is centered on 0.05 (median) with a 1% prior probability that it is smaller than 0.01 or larger than 2.5. Bernardinelli *et al.* (1995) also advocate the second prior, stating that it corresponds to a strong prior belief that the ratio of the 5% and 95% relative risks in the model with only independent random effects is approximately 1.85 when considering Poisson spatial models. Their choices are based on the ratio of the relative risk parameter at the 95th centile and the 5th centile, which has an easier interpretation than the corresponding variance parameter. Pasculto *et al.* (2000) comment that some of the priors referred to above (and a uniform prior on the interval (0,1)) cannot easily be fitted in analysis of disease mapping data.

In order to investigate the influence of hyperprior specifications for the binomial context, we carried out a sensitivity analysis with respect to the prior distributions for the spatial variance components σ_b^2 and σ_h^2, assuming a variety of different inverse gamma priors $IG(c, d)$, whose mode is $d/(c + 1)$. In particular, our experimental design used the following combinations: $(c, d) = (0.5, 0.0005)$, $(0.001, 0.001)$, $(0.01, 0.01)$, $(0.1, 0.1)$, $(2, 0.001)$, $(0.2, 0.0004)$, and $(10, 0.25)$, which are here denoted by A, B, C, D, E, F, and G, respectively. C and D are variants of prior B, with associated dispersion (larger than that of B) in increasing order; note, in addition, that B has much larger dispersion than prior A. The use of the inverse gamma with small values of $c = d$ provides a distribution with a very low probability on rather small values of the random effects standard deviations. Priors E and F correspond to distributions with the same mode as prior A, but with lower (E) and larger (F) dispersion. Prior G is quite concentrated and favours marked geographical variation (Bernardinelli *et al.*, 1995); it is the furthest from a noninformative setting.

For simplicity, we only show results for model $M4$ throughout this section. Apart from the prior settings A-G defined above, we also show several different settings which vary priors for the variances σ_b^2, σ_h^2 and σ_k^2, $k = 1, \ldots, 4$. Recall that these are variances of the spatially correlated random effect, the random effect modelling further excess heterogeneity, and the B-spline coefficients, respectively. The notation of a prior setting of AEA is to be interpreted as $\sigma_b^2 \sim IG(0.5, 0.0005)$, $\sigma_h^2 \sim IG(2, 0.001)$, and $\sigma_k^2 \sim IG(0.5, 0.0005)$. Similar interpretations apply for the other combinations of priors as itemized in Table 6. Recall that $\sigma_{b.tot}^2$ is the relative importance of the spatially correlated variance component when compared with the total spatial variance component, as defined previously. Estimates of the variance components σ_b^2, σ_h^2 and $\sigma_{b.tot}^2$, as well as associated standard deviations (s.d.), are provided in Table 6 for several variants of model $M4$ corresponding to the various choices of priors.

As shown in Table 6, generally there is fair correspondence in the posterior means of the variance components for the strata of males and females, as well as their standard deviations, across most choices of prior. Prior G is an exception, providing much smaller (largest) estimates of σ_b^2 and $\sigma_{b.tot}^2$ (σ_h^2) especially for the analysis of males. Increasing the prior mode of the variance hyperparameters results in larger estimates of the variance of the independent spatial random effects and smaller estimates of the variance of the spatially correlated random effects. In addition, prior E, whose mode is the same as prior A, also exhibits a distinct behaviour in the analysis of counts from females, increasing (decreasing) estimates of σ_b^2 (σ_h^2) in comparison with those from prior A. With these two priors, the standard deviation of the random effects is centered on 0.024 (E) and 0.161 (G) with lower than 0.05% prior probability that it is smaller than 0.01 or larger than 2.5. This is quite different from the prior assumptions using the priors B, C, D and F, where most of the prior mass is further away from zero. Prior A seems to provide a reasonable balance in allocating its prior mass between these two sets of priors.

Increasing the dispersion of the prior of each variance component (FAA, FAB, AFA, AFB) does not have a drastic effect on the estimates of σ_b^2 and σ_h^2 for males or females. On the other hand, decreasing the dispersion of the priors of the spatially correlated (EAA, EAB) and independent (AEA, AEB) components has a substantial decrease (increase) in the estimates of σ_b^2 (σ_h^2) and of σ_h^2 (σ_b^2), respectively. These differences of the estimates are not unexpected because decreasing the prior dispersion leads to inclusion of more prior information into the current setting. Gelman (2006) pointed

out that inference can become very sensitive for datasets in which low values of σ^2 are possible, suggesting a half-t distribution for the variance component instead of an inverse gamma prior in hierarchical models.

Since a main objective of this data analysis was to obtain estimates of relative spatial revascularization odds ($\exp(b_i + h_i)$), we also calculate the sum of the squared differences between the estimated odds obtained from prior A and each other prior setting defined above, focussing on the ten lowest and highest estimates for males and females as derived from the analysis using prior A. In Table 7, the associated values of this sum of squares were small, except for prior A versus priors EAA and EAB for females. We also calculate the corresponding sum of the absolute difference in the estimated odds ranks obtained from the use of prior A and each of the other prior settings (see the last columns of the Table 7). Prior G provided very different ranks for both genders, and priors E, EAA and EAB also produced large values of this sum for females, corresponding with results concerning the estimates of the variance component parameters in Table 6. Changing prior assumptions on the variance components does not have a considerable effect upon the estimates of the other parameters of interest.

6 Discussion

Models (2) and (3) provide smoothed estimates of the nonlinear overall and small-area temporal effects in mapping proportions over time and yield informative interpretations of the data. For the revascularization data analysis, they provided mechanisms for isolating small-area trends of importance in this study.

Using a fully Bayesian approach for the current spatiotemporal models, we are able to overcome inferential difficulties with the penalized quasi-likelihood method in the binomial context (MacNab and Dean (2001)). Corresponding marginal posteriors were readily available via MCMC methods. Studying the convergence of the samples obtained through diagnostic methods available in BOA program (Smith, 2004) indicates that convergence is somewhat slow and we recommend a cautious approach to assessing convergence here. Our sensitivity analysis using different priors for variance components pointed out that this hierarchical Bayesian spatiotemporal analysis for binomial data with splines can be quite robust with respect to hyperprior specification when the highest and lowest smoothed relative odds are under consideration.

Note though that certain priors with strong assumptions yield markedly differing results.

Acknowledgements

This paper was partially supported by FCT, GEOIDE, Merck Frosst, FRSQ and NSERC.

References

[1] Baladandayuthapani, V., Mallick, B.K. and Carrol, R.J. (2005). Spatially adaptive Bayesian penalized regression splines (P-splines). *Journal of Computational and Graphical Statistics*, **14**, 378-394.

[2] Banerjee, S., Carlin, B.P. and Gelfand, A.E. (2004). *Hierarchical Modeling and Analysis for Spatial Data*. Chapman & Hall/CRC.

[3] Bernardinelli, L., Clayton, D. and Montomoli, C., (1995). Bayesian estimates of disease maps: How important are priors?. *Statistics in Medicine*, **14**, 2411-2431.

[4] Besag, J. and Kooperberg, C.L. (1995). On conditional and intrinsic autoregressions. *Biometrika*, **82**, 733-746.

[5] Besag, J., York, J. and Mollié, A. (1991). Bayesian image restoration, with two applications in spatial statistics. *Annals of the Institute of Statistical Mathematics*, **43**, 1-59.

[6] Breslow, N.E. and Clayton, D.G. (1993). Approximate inference in generalized linear mixed models. *Journal of the American Statistical Association*, **88**, 9-25.

[7] Chen, M.-H., Shao, Q.-H., and Ibrahim, J.G. (2000). *Monte Carlo Methods in Bayesian Computation*. Sprnger-Verlag, New York.

[8] Gelman, A. (2006). Prior distributions for variance parameters in hierarchical models. *Bayesian Analysis*, to appear.

[9] Holmes, C.C. and Mallick, B.K. (2003). Generalized nonlinear modeling with multivariate free-knot regression splines. *Journal of the American Statistical Association*, **98**, 352-368.

[10] Kelsall, J.E. and Wakefield, J.C. (1999). Discussion of "Bayesian models for spatially correlated disease and exposure data", by Best, N.G., Waller, L.A., Thomas, A. Conlon, E.M., and Stern, R., in *Bayesian Statistics 6*, eds. Bernardo, J.M., Berger, J.O., Dawid, A.P., and Smith, A.F.M., Oxford University Press, Oxford.

[11] Knorr-Held, L. and Besag, J. (1998). Modelling risk from a disease in time and space. *Statistics in Medicine*, **17**, 2045-2060.

[12] Lawson, A.B., Biggeri, A., Böhning, D., Lesaffre, E., Viel J., and Bertollini, R. (eds) (1999). *Disease Mapping and Risk Assessment for Public Health*. Wiley, New York.

[13] Lin, X. and Breslow, N.E. (1996). Bias correction in generalized linear mixed models with multiple components of dispersion. *Journal of the American Statistical Association*, **91**, 1007-1016.

[14] MacNab, Y.C. (2003). Hierarchical Bayesian spatial modelling of small-area rates of non-rare disease. *Statistics in Medicine*, **22**, 1761-1773.

[15] MacNab, Y.C. and Dean, C.D. (2001). Autoregressive spatial smoothing and temporal spline smoothing for mapping rates. *Biometrics*, **57**, 949-956.

[16] Pampalon, R. and Raymond, G. (2000). A deprivation index for health and welfare planning in Quebec. *Chronic Disease in Canada*, **21**, 104-113.

[17] Pascutto, C., Wakefield, J.C., Best, N.G., Richardson, S., Bernardinelli, L., Staines, A. and Elliott, P. (2000). Statistical issues in the analysis of disease mapping data. *Statistics in Medicine*, **19**, 2493-2519.

[18] Smith, B.J. (2004). *BOA User Manual* (version 1.1.2). Department of Biostatistics, College of Public Health, University of Iowa.

[19] Spiegelhalter, D.J., Best, N.G., Carlin, B.P., and van der Linde, A. (2002). Bayesian measures of model complexity and fit. *Journal of the Royal Statistical Society B*, **64**, 583-639.

[20] Thomas, A., Best, N., Lunn, D., Arnold, R. and Spiegelhalter, D. (2004). *GeoBUGS User Manual* (version 1.2). Department of Epidemiology and Public Health, Imperial College, St Mary's Hospital London.

[21] Waller, L.A., Carlin, B.P., Xia, H. and Gelfand, A.E. (1997). Hierarchical spatio-temporal mapping of disease rates. *Journal of the American Statistical Association*, **92**, 607-617.

List of Figures

Rates	1993	1994	1995	1996	1997	1998	1999	2000
male	0.19	0.20	0.22	0.23	0.27	0.31	0.35	0.38
female	0.12	0.14	0.16	0.16	0.19	0.23	0.26	0.28

Table 1: Rates of revascularization at index hospitalization

Gender	Models defined from *logit* θ_{it}	$E(Q_P)$	$-\sum_i \log CPO_i$	deviance	DIC
male	$M1$: $\alpha_0+\beta t$	3367	4113.78	8220.62	8222.58
	$M2$: $\alpha_0+\beta t+\delta_i t+b_i+h_i$	1590	3312.53	6235.90	6448.68
	$M3$: $\alpha_0+S_0(t)+\delta_i t+b_i+h_i$	1564	3299.70	6212.31	6427.55
	$M4$: $\alpha_0+S_0(t)+S_i(t)+b_i+h_i$	1260	3158.51	5882.63	6199.37
female	$M1$: $\alpha_0+\beta t$	2035	2914.59	5830.71	5832.71
	$M2$: $\alpha_0+\beta t+\delta_i t+b_i+h_i$	1343	2641.53	5024.08	5201.24
	$M3$: $\alpha_0+S_0(t)+\delta_i t+b_i+h_i$	1338	2643.47	5020.39	5200.71
	$M4$: $\alpha_0+S_0(t)+S_i(t)+b_i+h_i$	1257	2620.24	4926.97	5154.76

Table 2: Comparison of the fits of sub-models of model (1)

Gender	Model	1993	1994	1995	1996	1997	1998	1999	2000
male	$M1$	0.213	0.248	0.287	0.333	0.386	0.448	0.520	0.603
	$M3$	0.223	0.249	0.271	0.301	0.351	0.428	0.515	0.580
	$M4$	0.227	0.246	0.267	0.297	0.347	0.421	0.511	0.593
female	$M1$	0.138	0.160	0.186	0.215	0.250	0.290	0.337	0.391
	$M3$	0.136	0.160	0.178	0.197	0.230	0.279	0.332	0.361
	$M4$	0.138	0.156	0.173	0.196	0.231	0.280	0.332	0.366

Table 3: Estimates of the overall odds of revascularization

Model	Gender	Parameter	mean	s.d.	median	95% credible interval
$M3$	male	σ_b^2	0.2056	0.0447	0.2057	(0.1198,0.2966)
		σ_h^2	0.0067	0.0077	0.0035	(0.0046,0.0089)
		$\sigma_{b.tot}^2$	0.9626	0.0498	0.9840	(0.8216,0.9990)
	female	σ_b^2	0.1835	0.0496	0.1840	(0.0818,0.2796)
		σ_h^2	0.0079	0.0097	0.0036	(0.0052,0.0115)
		$\sigma_{b.tot}^2$	0.9486	0.0762	0.9815	(0.7295,0.9990)
$M4$	male	σ_b^2	0.1053	0.0322	0.1019	(0.0479,0.1706)
		σ_h^2	0.0023	0.0034	0.0011	(0.0001,0.0094)
		$\sigma_{b.tot}^2$	0.9756	0.0401	0.9896	(0.9028,0.9996)
	female	σ_b^2	0.0698	0.0328	0.0673	(0.0001,0.1288)
		σ_h^2	0.0022	0.0035	0.0010	(0.0001,0.0083)
		$\sigma_{b.tot}^2$	0.9438	0.1409	0.9846	(0.7807,0.9995)

Table 4: Estimates of the variance components for models $M3$ and $M4$

Male		Female	
LHA	trend estimate	LHA	trend estimate
L'Amiante	0.843	L'Islet	0.859
Beauce-Sartigan	0.869	Manicouagan	0.864
Les Maskoutains	0.901	Vallée-de-l'Or	0.871
Bellechasse	0.907	Cote-Saint-Luc	0.887
Rivière-du-Loup	0.908	Lac-Etchemin	0.888
Sainte-Foy/Sillery	0.912	La Nouvelle-Beauce	0.900
Rouyn-Noranda	0.915	Pont-Viau	0.902
Montmagny	0.916	Basse Côte-Nord	0.905
Abitibi	0.923	L'Amiante	0.913
Quebec-Haute-Ville	0.924	Port-Cartier	0.914
⋮	⋮	⋮	⋮
Verdun	1.098	Les Laurentides	1.091
Les Laurentides	1.100	Lac Saint-Louis	1.095
Coaticook	1.102	Petite Patrie	1.097
Saint-Paul	1.102	Anjou	1.102
Pointe-aux-Trembles	1.103	Dollard-des-Ormeaux	1.107
Centre-de-la-Mauricie	1.115	Cap-de-la-Madeleine	1.117
Cap-de-la-Madeleine	1.138	Côte-des-Neiges	1.125
Asbestos	1.145	Métro	1.126
Gatineau	1.332	Gatineau	1.357
Hull	1.403	Hull	1.392

Table 5: Local health area (LHA) in increasing order of posterior mean estimates of the LHA temporal effects ($\exp(\delta_i)$) from model $M3$

Gender	Prior	σ_b^2		σ_h^2		$\sigma_{b.tot}^2$	
		mean	s.d.	mean	s.d.	mean	s.d.
male	A	0.1053	0.0322	0.0023	0.0034	0.9756	0.0401
	B	0.1057	0.0345	0.0055	0.0058	0.9443	0.0676
	C	0.0942	0.0335	0.0124	0.0072	0.8707	0.0920
	D	0.0894	0.0310	0.0272	0.0088	0.7527	0.0970
	E	0.1029	0.0316	0.0012	0.0019	0.9870	0.0227
	F	0.1070	0.0328	0.0035	0.0044	0.9646	0.0484
	G	0.0502	0.0160	0.0243	0.0063	0.6629	0.1012
	AEA	0.1095	0.0323	0.0008	0.0009	0.9917	0.0097
	AEB	0.1066	0.0328	0.0009	0.0010	0.9908	0.0109
	AFA	0.1051	0.0341	0.0036	0.0047	0.9625	0.0542
	AFB	0.1029	0.0326	0.0034	0.0046	0.9642	0.0542
	EAA	0.0920	0.0307	0.0028	0.0045	0.9651	0.0648
	EAB	0.0889	0.0306	0.0031	0.0043	0.9601	0.0696
	FAA	0.1091	0.0327	0.0026	0.0034	0.9744	0.0366
	FAB	0.1096	0.0330	0.0024	0.0033	0.9759	0.0362
female	A	0.0698	0.0329	0.0022	0.0035	0.9438	0.1409
	B	0.0711	0.0311	0.0046	0.0048	0.9276	0.0862
	C	0.0641	0.0307	0.0103	0.0065	0.8348	0.1321
	D	0.0687	0.0281	0.0250	0.0084	0.7141	0.1119
	E	0.1065	0.0509	0.0010	0.0015	0.9816	0.0578
	F	0.0706	0.0319	0.0032	0.0043	0.9451	0.0824
	G	0.0383	0.0132	0.0252	0.0066	0.5928	0.1087
	AEA	0.0728	0.0315	0.0009	0.0012	0.9820	0.0429
	AEB	0.0664	0.0328	0.0009	0.0011	0.9719	0.0927
	AFA	0.0700	0.0325	0.0031	0.0046	0.9429	0.0958
	AFB	0.0659	0.0327	0.0030	0.0043	0.9376	0.1087
	EAA	0.0126	0.0247	0.0080	0.0106	0.4216	0.3670
	EAB	0.0071	0.0175	0.0074	0.0100	0.3865	0.3335
	FAA	0.0756	0.0318	0.0021	0.0030	0.9670	0.0532
	FAB	0.0706	0.0316	0.0024	0.0035	0.9573	0.0736

Table 6: Estimates of the spatial variance components based on model $M4$ with different inverse gamma hyperpriors

Prior	Sum of squares of difference in odds estimates				Sum of absolute values of difference in rank estimates			
	Male		Female		Male		Female	
	bottom 10	top 10	bottom 10	top 10	bottom 10	top 10	bottom 10	top 10
B	0.0005	0.0010	0.0005	0.0010	2	2	0	2
C	0.0018	0.0024	0.0013	0.0024	4	10	2	12
D	0.0089	0.0186	0.0150	0.0283	6	14	19	21
E	0.0007	0.0002	0.0604	0.0467	2	2	61	44
F	0.0003	0.0006	0.0002	0.0003	2	0	2	4
G	0.0148	0.0088	0.0420	0.0413	10	18	57	45
AEA	0.0002	0.0002	0.0002	0.0001	0	2	5	2
AEB	0.0001	0.0002	0.0016	0.0017	2	2	6	2
AFA	0.0002	0.0003	0.0002	0.0001	0	2	5	6
AFB	0.0002	0.0002	0.0006	0.0004	2	2	0	2
EAA	0.0012	0.0035	0.1844	0.1974	2	2	28	27
EAB	0.0025	0.0063	0.2457	0.2597	2	2	28	27
FAA	0.0003	0.0009	0.0013	0.0013	2	2	5	6
FAB	0.0002	0.0007	0.0002	0.0003	2	2	5	2

Table 7: Sum of squares of the differences in the estimates and sum of the absolute values of the difference in the ranks of the estimates of the revascularization odds based on model $M4$ with prior A and those obtained with other priors by gender

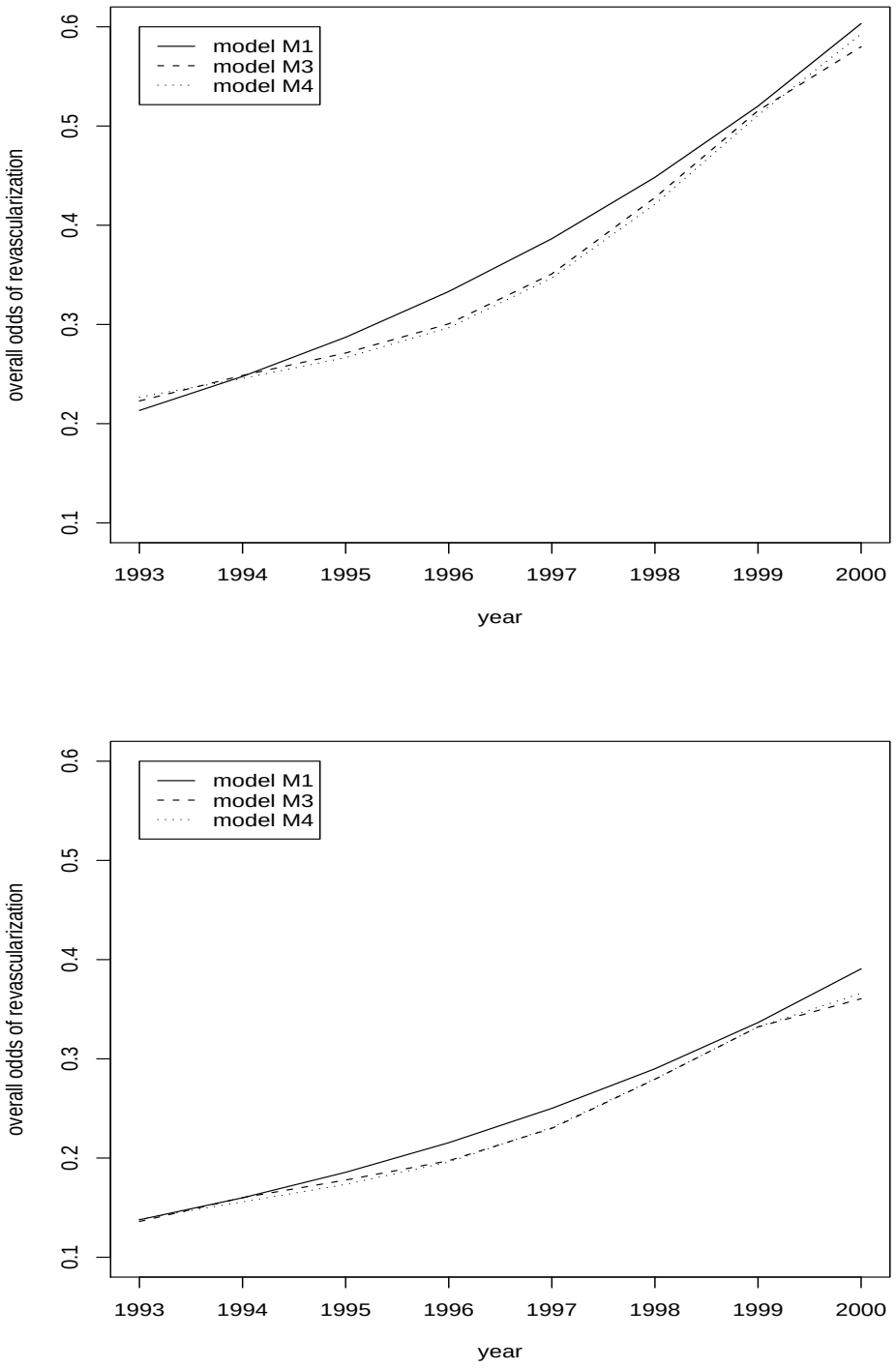

Figure 1: Overall odds of revascularization for males (top) and females (bottom)

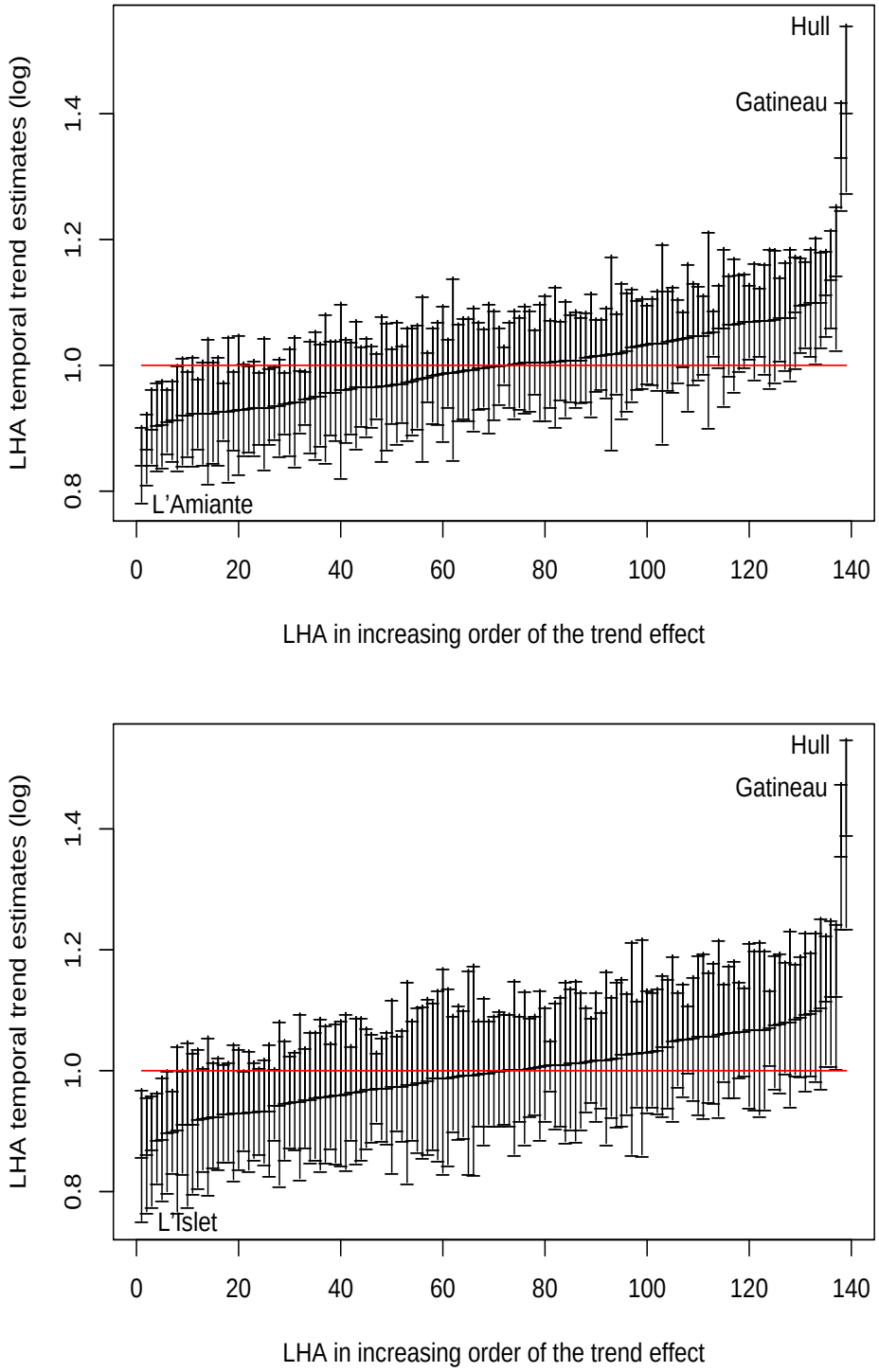

Figure 2: Credible intervals of the LHA temporal trend in revascularization odds for males (top) and females (bottom) based on model $M3$

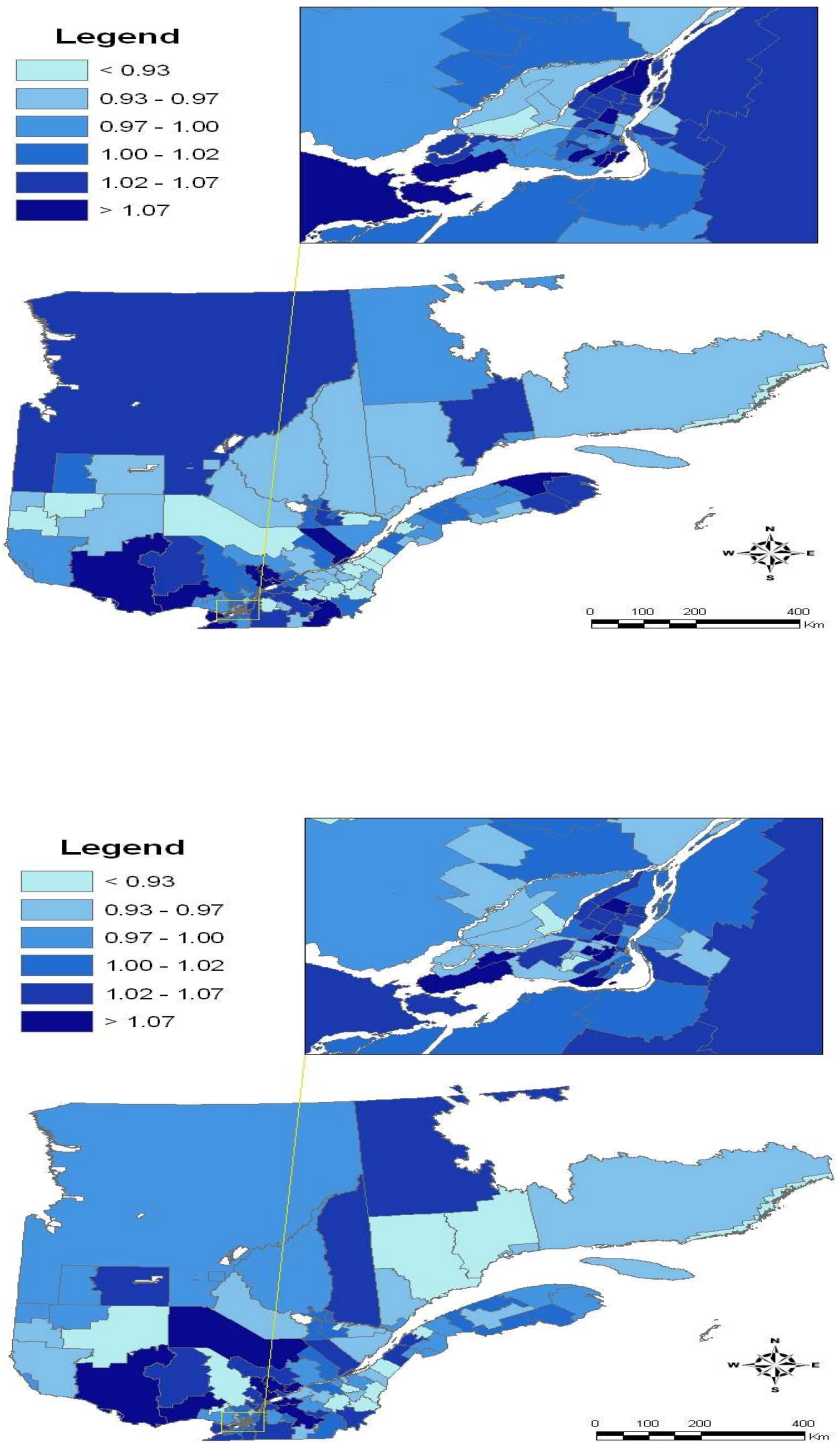

Figure 3: Maps of the linear LHA temporal trend estimates in revascularization odds for males (top) and females (bottom) based on model $M3$

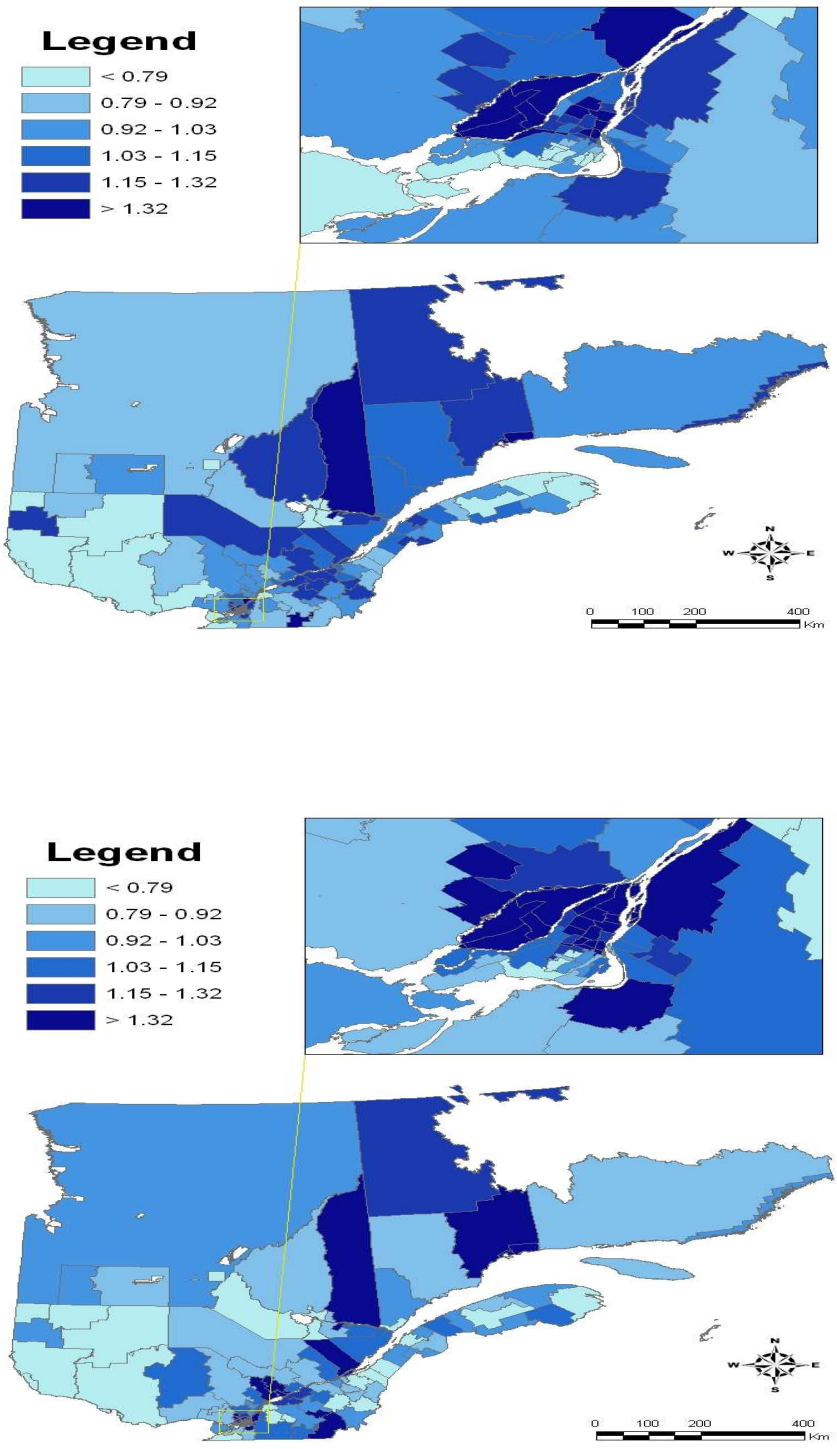

Figure 4: Maps of the revascularization odds estimates for males in 1993 (top) and 2000 (bottom) based on model $M4$

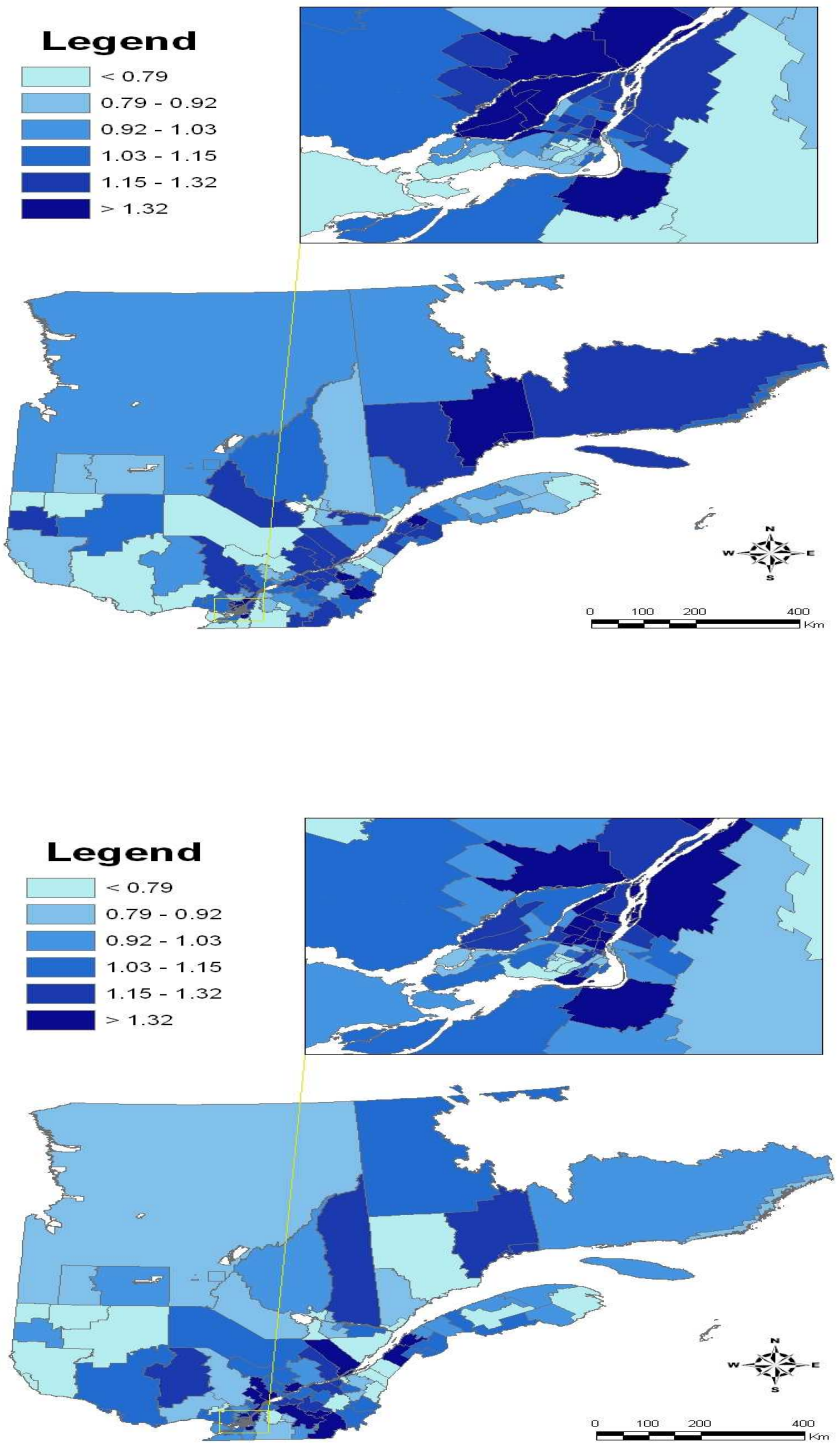

Figure 5: Maps of the revascularization odds estimates for females in 1993 (top) and 2000 (bottom) based on model $M4$

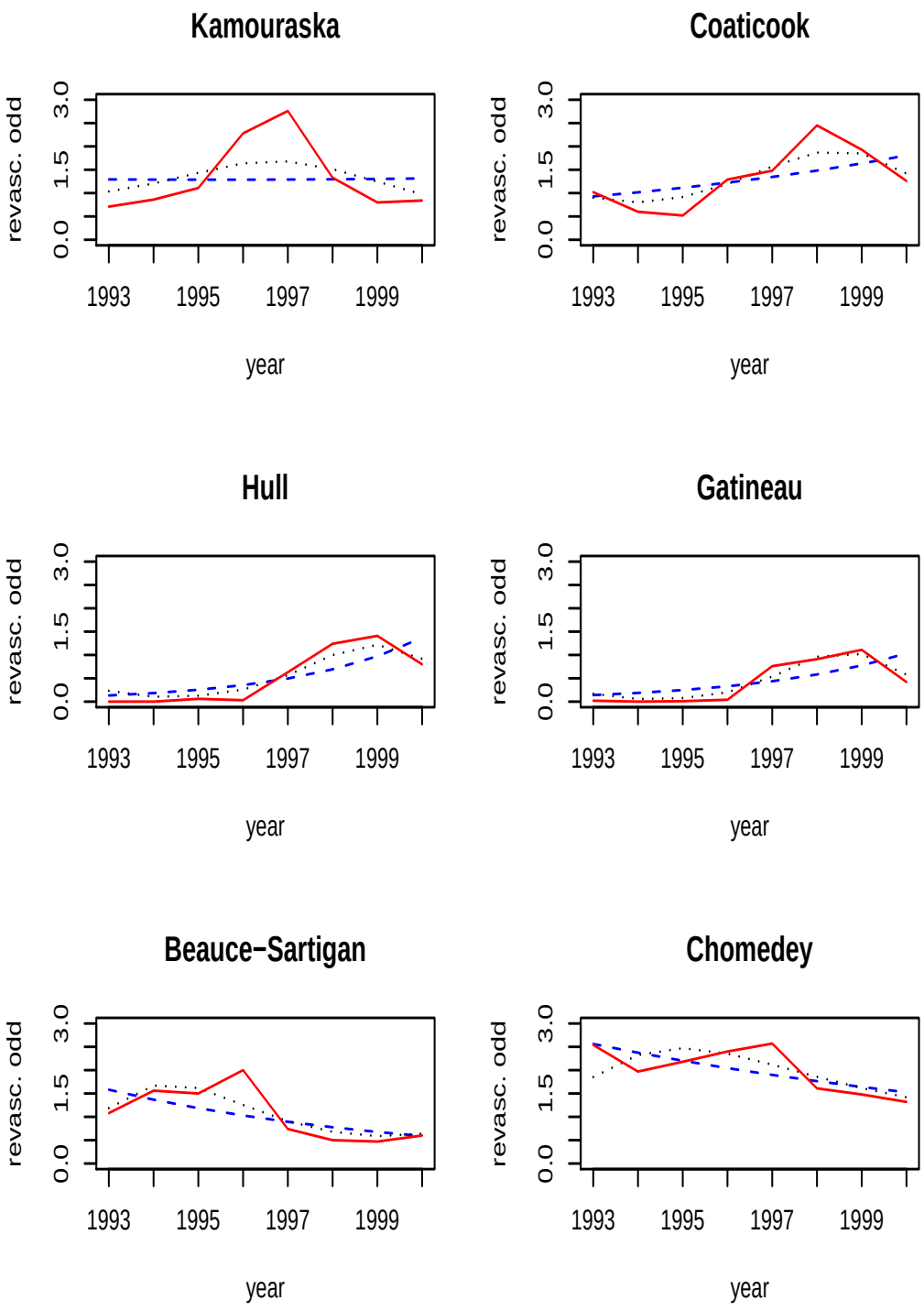

Figure 6: Plots of the standardized crude odds (—) for specific local health areas by year for males and estimated revascularization odds based on model $M3$ (- - -) and model $M4$ ($\cdots$)

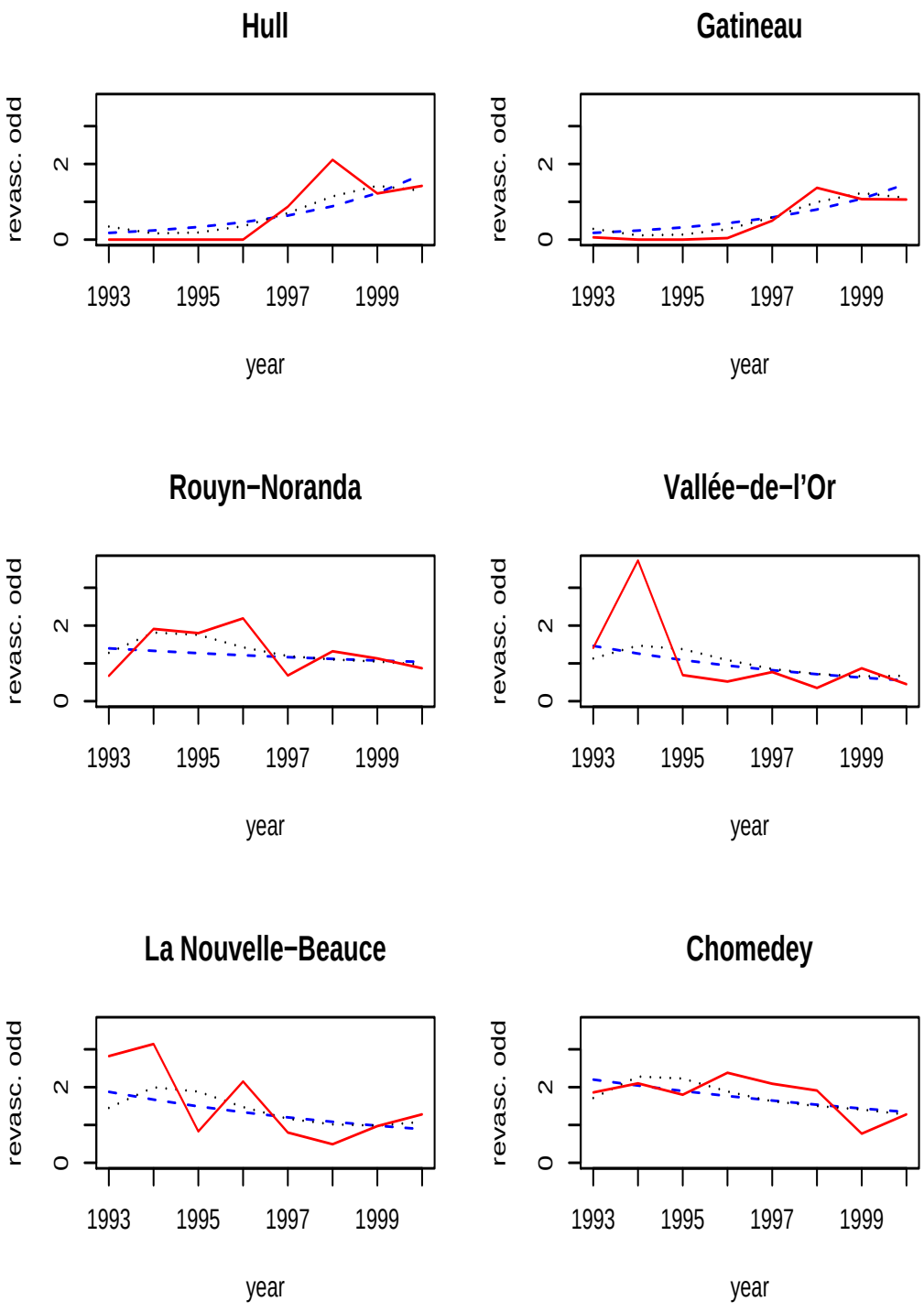

Figure 7: Plots of the standardized crude odds (—) for specific health areas by year for females and estimated revascularization odds based on model $M3$ (- - -) and model $M4$ ($\cdots$)

Recent Preprints

2006

1/06 Carlos A. A. Florentino. Invariants of 2×2 matrices, irreducible SL(2,C) characters and the Magnus trace map. 16pp.

2005

1/05 Natasha Samko. *On non-equilibrated almost monotonic functions of the Zygmund-Bari-Stechkin class*. 18pp.

2/05 Natasha Samko. *Singular integral operators in weighted spaces of continuous functions with non-equilibrated continuity modulus*. 26pp.

3/05 Pedro Resende. *Étale groupoids and their quantales*. 62pp.

4/05 M. Casquilho, M. Constantino, M. C. Morais. *Sobre a amostragem de aceitação para a variável gaussiana inversa*. 14pp.

5/05 M. C. Morais, A. Pacheco. *Assessing the impact of head starts in the performance of one-sided Markov-type control schemes*. 23pp.

6/05 L. P. Castro, F.–O., Speck, F. S. Teixeira. *Mixed boundary value problems for the Helmholtz equation in a quadrant*. 42pp.

7/05 M. A. Bastos, P. A. Lopes, A. M. Santos. *Periodic oblique derivative and Neumann boundary-value problems: the two straight line approach*. 22pp.

8/05 Natasha Samko. *On compactness of integral operators with a generalized weak singularity in weighted spaces of continuous functions with a given continuity modulus*. 25pp.

9/05 M. C. Morais, A. Pacheco, W. Schmid. *On the stochastic behaviour of the run length of EWMA control schemes for mean of correlated output in the presence of shifts in* s. 20pp.

10/05 R. Coutinho, B. Fernandez, R. Lima, A. Meyroneinc. *Discrete time piecewise affine models of genetic regulatory networks*. 37pp.

11/05 Yu. I. Karlovich and Luís Pessoa. *C*-Algebras of Bergman Type Operators with Piecewise Continuous Coefficients*. 53pp.

12/05 Jean-François Babadjian and Margarida Baía. *Multiscale nonconvex relaxation and application to thin films*. 46pp.

13/05 L.P. Castro, R. Duduchava and F.-O. Speck. *Asymmetric Factorizations of Matrix Functions on the Real Line*. 24pp.

The Mathematics Department of Instituto Superior Técnico offers a preprint series open to its faculty, PhD students and visitors who wish to make available a preview of their work before formal publication. Starting with issue 11/05 the preprints are only available in electronic (PDF) format from

http://preprint.math.ist.utl.pt/?serie=dmist

The preprints are the exclusive responsability of their authors. This preprint series does not purport to be complete with respect to all faculty members, students and visitors who may offer preprints from other locations.